Journal of Atmospheric and Solar-Terrestrial Physics 121 (2014) 50–58

Contents lists available at ScienceDirect

Journal of Atmospheric and Solar-Terrestrial Physics

journal homepage: www.elsevier.com/locate/jastp

Cosmogenic production and climate contributions to nitrate record in the TALDICE Antarctic ice core

S. Poluianov [a,*], R. Traversi [c], I. Usoskin [a,b]

[a] Department of Physics, FI-90014, University of Oulu, Finland
[c] Department of Chemistry "Ugo Schiff", University of Florence, via della Lastruccia, I-50019 Sesto Fiorentino, Italy
[b] Sodankylä Geophysical Observatory (Oulu unit), University of Oulu, FI-90014, Finland

ARTICLE INFO

Article history:
Received 18 May 2014
Received in revised form
15 September 2014
Accepted 24 September 2014
Available online 28 September 2014

Keywords:
Solar activity
Nitrate
Holocene
TALDICE

ABSTRACT

This paper presents the results of a comparative wavelet coherence analysis of a multimillennial nitrate record with a number of climatic and solar activity proxies. Distinguishing between these factors is important in the view of a possibility of nitrate deposited in a polar region to represent galactic cosmic ray flux and, consequently, solar activity. We used the data from the TALDICE drilling project (Talos Dome, Antarctica), which covers the age range 12,000–700 BP (years before present, i.e. before 1950) and includes records of nitrate as well as climatic proxies, such as Na^+, Ca^{2+}, MSA (methanesulphonic acid), $\delta^{18}O$, SO_4^{2-}. The solar activity series is represented by reconstructions of the heliospheric modulation parameter from the ^{14}C and ^{10}Be data. We found (1) a confirmation of multimillennial relation between nitrate and galactic cosmic ray flux; (2) no clear signature of long-term variations of nitrate transport from lower latitudes. We suggest that variations in the nitrate record in the time scale of hundreds–thousands years are most likely caused by local production, deposition and post-deposition processes.

1. Introduction

It is important for many reasons to reconstruct the variability of solar activity on the long-term scale extending over centennia and millennia. The only established quantitative way to reconstruct solar activity in the past, before direct solar observations, is related to the use of a proxy which corresponds to the flux of galactic cosmic rays impinging the Earth. Galactic cosmic ray flux is modulated by solar activity in the heliosphere and is roughly inversely proportional to it. The intensity of cosmic rays is recorded in concentration of the so-called cosmogenic isotopes, primarily ^{14}C and ^{10}Be, measured in natural independently dated archives, such as tree trunks or ice cores (e.g., Beer et al., 2012; Usoskin, 2013). In addition to these well-established cosmogenic nuclear proxies of solar activity, a chemical tracer was recently proposed (Traversi et al., 2012; Soon et al., 2014) — nitrate (NO_3^{α}) measured in an Antarctic ice core. In particular, it was shown that the nitrate record from the TALDICE ice core depicts significant coherence with the cosmogenic radiocarbon ^{14}C on the time scale of ten millennia, which was interpreted as an evidence for a dominant solar signal in the nitrate production. Accordingly, the polar nitrate was proposed as a potential proxy for solar activity on different timescales (from decadal to multi-millennial). We note that the relation between nitrate and solar activity proposed by Traversi et al. (2012) is caused by the variability of galactic cosmic rays which is different from the disputable response of polar nitrate to major solar energetic particle events (McCracken et al., 2001; Palmer et al., 2001; Kepko et al., 2009; Wolff et al., 2008, 2012). This is a new feature as typically nitrate is used as a tracer of natural and anthropogenic nitrogen species emissions (e.g., Mayewski et al., 1986, 1990; Legrand and Mayewski, 1997).

If proven to be a reliable proxy, the new chemical tracer would be a useful addition to the traditional cosmogenic radionuclide proxies. Nitrate, in contrast to cosmogenic radionuclides, is not purely cosmogenic — it is appreciably controlled by a number of terrestrial sources and processes not related to solar activity. Here we try to disentangle production and transport effects in the nitrate using an empirical analysis of the mutual relations between NO_3^{α} and other chemical tracers, measured in the same TALDICE core.

2. Data and method

Nitrate ions (NO_3^{α}) in Antarctic snow/ice represent mainly deposited gaseous acid HNO_3, the ultimate product of reactions with nitrogen oxides (NO_x) in the atmosphere (e.g., Legrand and Kirchner, 1990; Delmas, 1992). The sources of nitrate and/or its

* Corresponding author.
E-mail address: stepan.poluianov@oulu.fi (S. Poluianov).

http://dx.doi.org/10.1016/j.jastp.2014.09.011
1364-6826/

precursors include (1) the photochemical dissociation of N_2O occurring in the stratosphere, that is mainly responsible for production of reactive NO_x in the stratosphere and their further downwelling to the troposphere (e.g., Legrand and Kirchner, 1990); (2) production of several nitrogen species (NO_x, peroxyacetyl nitrates) in the low and middle latitude areas by lightnings (e.g., Wolff, 1995), (3) biomass burning and recent (4) anthropogenic activity (and references therein Grannas et al., 2007), and, finally, (5) the re-emission from the snowpack of volatile HNO_3 (e.g., Weller and Wagenbach, 2007) or through photolysis-emission of NO_x and subsequent oxidation in the atmosphere (Grannas et al., 2007). As concerning the NO_x production in the stratosphere, a very important source is related to interactions of high-energy particles, namely galactic cosmic rays and solar energetic particles with the ambient air (e.g., Vitt and Jackman, 1996). In contrast to the lightning-related source this one is stronger in polar regions with weaker or no geomagnetic shielding. Here we focus on the south polar region where the local production of NO_3^- by lightnings is negligible but its influence can be still important due to transport of NO_3^- from lower latitudes.

In order to study the climate influence on NO_3^- we compare it with a number of available data series which are strongly subjected to various climatic factors (temperature, air transport, etc.). We use the data that were obtained in the framework of the Talos Dome Ice Core drilling project (TALDICE), where an ice core covering a hundred of thousands of years was obtained. The drilling site is located in Central Antarctica (72°49′S, 159°11′E, 2315 m above sea level). The data represent age-concentration series that cover the age range from 12,000 to 700 BP (years before present, i.e. before 1950) with dating uncertainties keeping below 150 years in the late Holocene, back to 4500 BP (Bazin et al., 2013). Since the dominant type of NO_3^- deposition at Talos Dome is dry (Traversi et al., 2012), the deposition flux (i.e. concentration times snow accumulation rate) is generally more suitable than the concentration to derive the quantity of each component actually deposited onto the ice sheet, as usually accomplished when dry deposition is dominant with respect to wet deposition (e.g., EPICA Community Members, 2004). Nonetheless, introducing a parameter (deposition flux) which is not directly measured but calculated from the measured concentration by applying a suitable flow model and absolute temporal horizons (Bazin et al., 2013) carries an additional uncertainty which has to be taken into account when discussing the variability of the chemical data series. The choice between a data series obtained by direct measurements (concentrations) but not directly related to atmospheric depositions and a data series directly related to depositions (flux) but obtained by introducing another calculated parameter, not measured parameter (accumulation rate), is not straightforward. In such a case, considering that this work focuses on the relative variability, rather than on the absolute atmospheric concentrations, and keeping in mind that the accumulation rate was nearly constant during the Holocene, we chose to consider the concentration series as more robust. Moreover, the possible tuning effect of different accumulation rates on concentrations might be significant when these series are compared with an "external" series with independent dating, but not for different tracers obtained from the same ice core.

We consider the following substances whose strong relations with some climatic parameters make them useful markers of aerosol production and/or transport processes:

- sodium Na^+ is a tracer of sea salt supply to the deposition site;
- calcium Ca^{2+} generally reflects dust aerosol transported from areas with open soil;
- methanesulphonic acid $CH_3SO_3^-$ (MSA henceforth) represents phytoplankton activity in the ocean;
- relative concentration of ^{18}O isotope ($\delta^{18}O$ henceforth) is an index of the air temperature at the deposition site;
- non-sea-salt sulphate $nssSO_4^{2-}$ is mainly driven by the phytoplankton activity in the ocean as well as by volcanic activity and anthropogenic SO_2 emissions with a small contribution from mineral dust (e.g., gypsum).

In order to exclude the influence of sea spray on the measured SO_4^{2-} we calculate the non-sea-salt value using the following equation (Traversi et al., 2004):

$$[nssSO_4^{2-}] = [SO_4^{2-}] - 0.253[Na^+], \quad (1)$$

where all the values represent mass concentrations in the unit of μg/L.

Since many of those substances are produced outside of the Antarctic ice sheet, their concentrations in the TALDICE ice core are strongly influenced by the air transport factor.

As an index of cosmic ray variability we use heliospheric modulation parameter ϕ (see Usoskin et al., 2005 for definition). Because of the inverse relation between ϕ and the cosmogenic production rate in the atmosphere, for convenience we use inverse values of modulation parameter, denoted henceforth as Φ. Thus, an increase of the inverse modulation parameter Φ corresponds to an increase of the cosmic ray flux and, consequently, an increase of the cosmogenic production rate. The series of ϕ is based on the globally averaged ^{14}C data (INTCAL09 project, see Reimer et al., 2009) and is converted into the cosmic ray modulation using a model by Kovaltsov et al. (2012). This series covers the same time range as the TALDICE series. The other one is based on measurements of ^{10}Be in a Greenland ice core in the framework of GRIP project (Yiou et al., 1997) and converted into the cosmic rays modulation by Steinhilber et al. (2008). This series is somewhat shorter, covering the period from 9300 to 700 BP.

Since the data series are essentially non-stationary and varying on different time scales, the conventional bivariate correlation analysis is not appropriate. Accordingly, we study relations between series using the method of wavelet coherence (e.g., Torrence and Compo, 1998; Lachaux et al., 2002) which allows one to disentangle the relation between data series in both temporal and frequency domains. Namely, we apply the Matlab-based software package originally developed by Grinsted et al. (2004). The original package estimates the significance of coherence using an assumption of a red noise model of the signal, which may essentially overestimate the significance (Usoskin et al., 2006; Poluianov and Usoskin, 2014). In order to be on a safe side, we apply a more conservative Monte-Carlo non-parametric random-phase method (Ebisuzaki, 1997) for the estimate of significance. Its application to the wavelet coherence procedure is described, e.g., by Traversi et al. (2012). The original code by Grinsted et al. (2004) was modified accordingly. Before the analysis, all data series were standardized, viz. normalized to the mean, and divided by the standard deviation, and additionally low-pass filtered by the rectangular window in frequency domain with the cutoff frequency 0.01 $year^{-1}$. We used the following parameters of the wavelet coherence computation: the Morlet wavelet basis with $\omega_0 = 3$; statistical significance of the results was calculated for 1000 Monte-Carlo runs using the non-parametric random-phase method. In addition to the conventional 2D coherence (in time and frequency domains) we also computed the time-averaged coherence, considering also the relative phase of the signals (see details in Traversi et al., 2012).

All the plots are arranged in the same manner as described in the caption of Fig. 1.

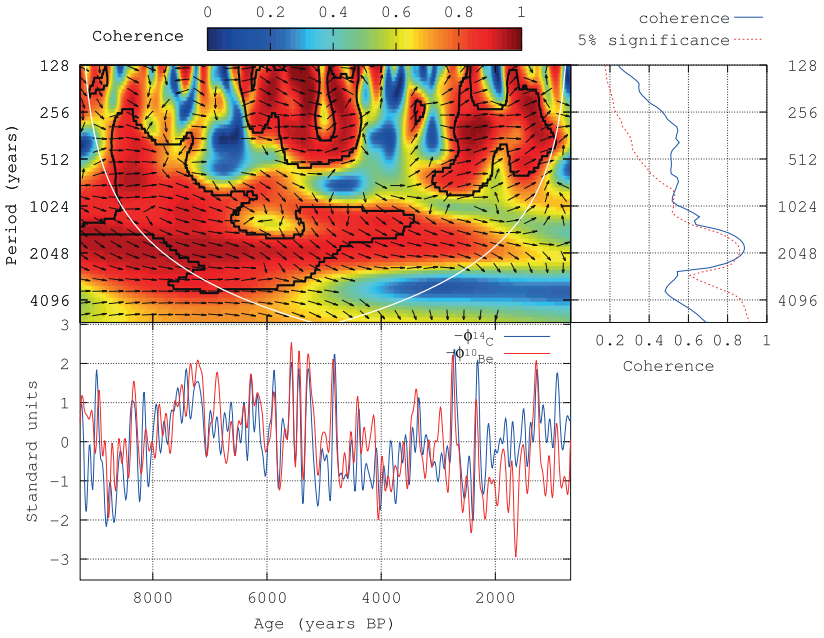

Fig. 1. Comparison of inverse modulation parameters $-\phi$ reconstructed from the records of cosmogenic isotopes ^{14}C and ^{10}Be. The top-left panel shows the wavelet coherence between the series. Colours represent the coherence value (see the colour bar). Arrows indicate the phase difference (right-pointing arrows correspond to 0°, up-pointing arrows — 90°, etc.). Black contours bound areas with the statistical significance of the coherence better than 5%. The white lines in the wavelet coherence plot indicate a cone of influence, an area subjected to the edge effect. The top-right panel shows the time-averaged coherence and the corresponding 5% significance estimated by the non-parametric random-phase method (Ebisuzaki, 1997). The bottom panel depicts time variations of the series. (For interpretation of the references to colour in this figure caption, the reader is referred to the web version of this paper.)

3. Results and discussion

In this section we discuss the results of comparisons between NO_3^- and the substances/proxies that are described in Section 2. First, we denote the following local terms: the short-period range is 128–512 years, the mid-period range is 512–2048 years, and the long-period range is 2048 years and longer. We do not consider variations with periods shorter than 128 years because of dating errors in the data sets.

3.1. Nitrate and cosmic ray flux

Firstly, we intercompare the two series of the heliospheric modulation parameter ϕ based on ^{14}C and ^{10}Be in order to check their ability to represent cosmic ray flux as a common production factor (Fig. 1).

A visual inspection of the two time series (the bottom panel) confirms a good agreement between them except for the interval of 675–2500 BP. Short- and mid-term variations are generally also

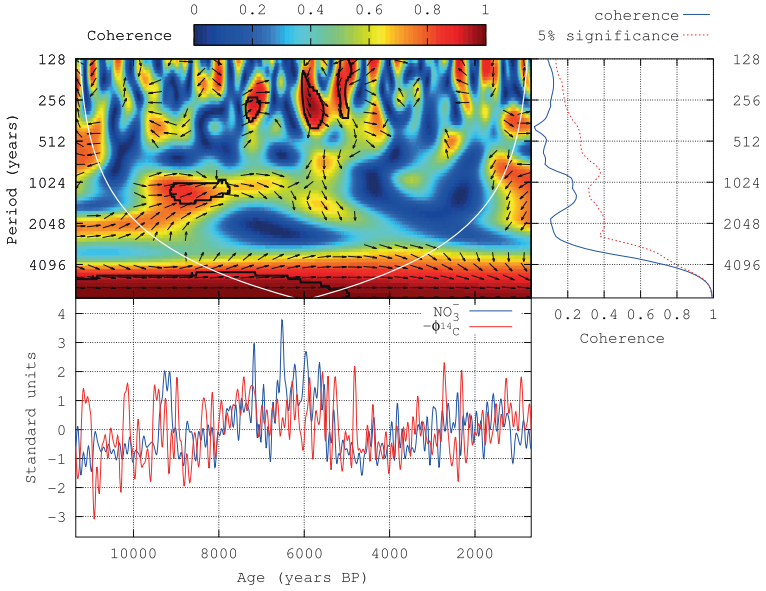

Fig. 2. Similar to Fig. 1 but for the concentration of NO_3^- and inverse modulation parameter $-\phi$ reconstructed from the records of cosmogenic isotope ^{14}C.

coincident. Both series have a number of strong dips, e.g., at 8320, 5570, 4840, 2750 BP, corresponding to Grand Minima (cf. Usoskin et al., 2007). The top panels present patterns of coherence between the series. Overall, the good agreement between the data is confirmed by a relatively high coherence, but its distribution in the time-period space is nonuniform. The high and statistically significant coherence is observed at short- and mid-period ranges but not at long-period range (cf. Usoskin et al., 2009). One can see that while the mid- and long-period coherence is low at the interval 5000–675 BP there are two "spots" of very high short-period coherence. The disagreement between the $\mathscr{Ab}^{14}C$ and $\mathscr{Ab}^{10}Be$ series in long-time scale was found earlier (e.g., Vonmoos et al., 2006; Usoskin et al., 2009).

We ascribe the high coherence found in short- and mid-period ranges by cosmic ray flux that drives production of both isotopes. The disagreement at long-time scale can be caused by variation of some parameters in the production–transport–deposition chain of ^{14}C and/or ^{10}Be.

Because of the weak relation in long-time scale either $\mathscr{Ab}^{14}C$ and/or $\mathscr{Ab}^{10}Be$ series can be distorted in the sense of the long-term cosmic rays variability, and the extraction of the true cosmic ray behaviour from those data series is not trivial (Steinhilber et al., 2012). Therefore, we compare nitrate with each of cosmogenic isotopes separately assuming that each of them is mainly driven by cosmic ray flux but may also contain a climate-related signal.

The next pair to compare is $NO_3^{\mathscr{G}}$ and $\mathscr{Ab}^{14}C$ (Fig. 2). The main feature here is a statistically significant very high (up to 0.99, see the right panel of Fig. 2) and in-phase coherence at long-period range. In contrast, at the short- and mid-periods, there are only a few significant "spots" of high coherence: at 9000–8000 BP for periods about 1024 years, at 7100–6600 BP, and at 6000–5800 BP for periods about 256 years. They are short-term and look like coincidences of variations even with a good significance.

Overall, the coherence at short- and mid-periods is low and it can probably be explained by climatic influence, while highly coherent long-period variations of $NO_3^{\mathscr{G}}$ and $\mathscr{Ab}^{14}C$ are most likely caused by cosmic ray flux, directly affecting their production.

This result is in quantitative agreement with the same comparison done earlier by Traversi et al. (2012). A minor difference can be explained by the discrepancy in details of the computation procedure.

Comparison of $NO_3^{\mathscr{G}}$ and $\mathscr{Ab}^{10}Be$ is presented in Fig. 3. Unlike the previous case with $\mathscr{Ab}^{14}C$, $NO_3^{\mathscr{G}}$ and $\mathscr{Ab}^{10}Be$ are weakly coherent at all ranges of periods. Nevertheless, one can see an interval of common long-period behaviour of the two series ca. 9400–7000 BP. During the rest of the time the long-period coherence is very low. At short- and mid-period ranges there are a few small "spots" of relatively high coherence. Their phases have values near $+90°$ or $-90°$ and are strongly variable. Detailed examination of the time series suggests that these "spots" cannot indicate any real relation between the data sets, but are accidental.

Thus, the result of the wavelet coherence analysis in Fig. 3 leads to the conclusion that there is no significant relation between $NO_3^{\mathscr{G}}$ and $\mathscr{Ab}^{10}Be$. This distinction can be probably caused by local features of transport and/or deposition of ^{10}Be in Greenland. The lack of short- and mid-period relation in the $NO_3^{\mathscr{G}}$ vs. $\mathscr{Ab}^{10}Be$ pair as well as in the $NO_3^{\mathscr{G}}$ vs. $\mathscr{Ab}^{14}C$ pair on the one hand, and the good short- and mid-period coherence between $\mathscr{Ab}^{14}C$ and $\mathscr{Ab}^{10}Be$ on the other hand suggests that the $NO_3^{\mathscr{G}}$ series may be affected by noncosmogenic factors, most likely of climatic nature.

In an attempt to understand the influence of that kind of process on $NO_3^{\mathscr{G}}$ deposition we compare it with a number of climatic markers described in Section 2.

3.2. $NO_3^{\mathscr{G}}$ *vs.* $nssSO_4^{2\mathscr{G}}$ *and MSA*

The comparison of $NO_3^{\mathscr{G}}$ and $nssSO_4^{2\mathscr{G}}$ is shown in Fig. 4. The wavelet analysis shows significant coherence for long- and mid-period variations of the series. However, the phase shift of about $-45°$ at long-period range and visual inspection of the two series point to the lack of real long-term relation between $NO_3^{\mathscr{G}}$ and $nssSO_4^{2\mathscr{G}}$. On the contrary, the mid-period range has three "spots" of high and in-phase coherence (ca. 10,500–8500, 8000–7000 and 3000–2000 BP). This indicates sporadic relation between the series. A number of coincident peaks (in the bottom panel), reflected as small "spots" of high coherence (in the top-left panel), are likely due to a random occurring co-variability and not to a common driver in production and/or transport, as suggested by their short duration and random relative phase.

The discrepancy between $NO_3^{\mathscr{G}}$ and $nssSO_4^{2\mathscr{G}}$ at periods longer than 4000 years can be explained in the view that $NO_3^{\mathscr{G}}$ production is dominated by galactic cosmic rays at long period range (see Section 3.1), while $nssSO_4^{2\mathscr{G}}$ is totally independent on it. The

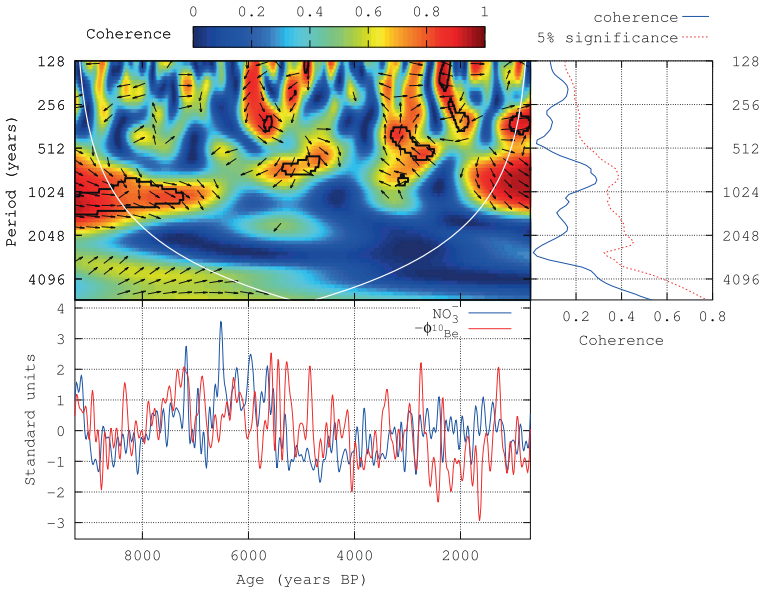

Fig. 3. Similar to Fig. 1 but for the concentration of $NO_3^{\mathscr{G}}$ and inverse modulation parameter $-\phi$ reconstructed from the records of cosmogenic isotope ^{10}Be.

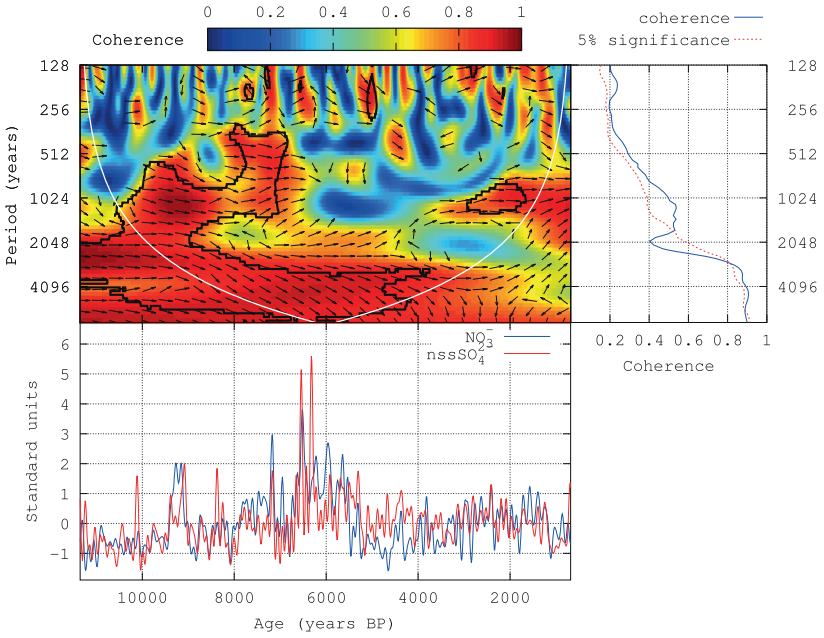

Fig. 4. Similar to Fig. 1 but for the concentrations of $NO_3^{\mathcal{G}}$ and no-sea-salt $SO_4^{2\mathcal{G}}$.

significant coherence at other period ranges can be caused by common formation processes from already present precursors in gas-phase (NO_x and SO_2 or dimethyl sulphoxide (DMSO) for $NO_3^{\mathcal{G}}$ and $nssSO_4^{2\mathcal{G}}$, respectively), or by common transport processes from the middle and low latitudes. Concerning the first option, it is reasonable to assume that the efficiency of atmospheric oxidation of $NO_3^{\mathcal{G}}$ and $nssSO_4^{2\mathcal{G}}$ precursors is somewhat higher in conditions of higher solar irradiation, and this may provide a link between the two parameters. For instance, a common behaviour at seasonal scale has been found in several Antarctic sites by the analysis of snow pits and firn cores, even allowing us to perform a relative dating on the basis of a clear seasonal pattern (e.g., Severi et al., 2009). The seasonality of $nssSO_4^{2\mathcal{G}}$ has always been ascribed to the annual variations of biogenic productivity (blooming in summer) whereas the seasonality of $NO_3^{\mathcal{G}}$ has been so far overlooked and not clearly explained despite being used in several works for ice dating via annual layer counting of single parameters or via a multi-parametric approach (Wolff, 1995; Traufetter et al., 2004; Severi et al., 2009). The dependence of $NO_3^{\mathcal{G}}$ and $nssSO_4^{2\mathcal{G}}$ on the solar irradiation can be analysed by intercomparison with MSA, a proxy of biogenic productivity (e.g., Saltzman et al., 2006) and, indirectly, of solar irradiation. Here we should note that other climatic factors such as sea-ice extent and atmospheric circulation modes (e.g., South Oscillation Index (SOI) and Southern Annual Mode (SAM)) might affect MSA budget and temporal trends in Antarctic sites relatively close to the coast, like Talos Dome (Becagli et al., 2009; Curran et al., 2003).

The wavelet coherence and the time variations of $NO_3^{\mathcal{G}}$ and MSA are presented in Fig. 5. There are several relatively large areas of statistically significant high coherence in long-, mid- and short-period ranges. However the relative phases of the "spots" vary significantly. The area of high coherence at the long-period range

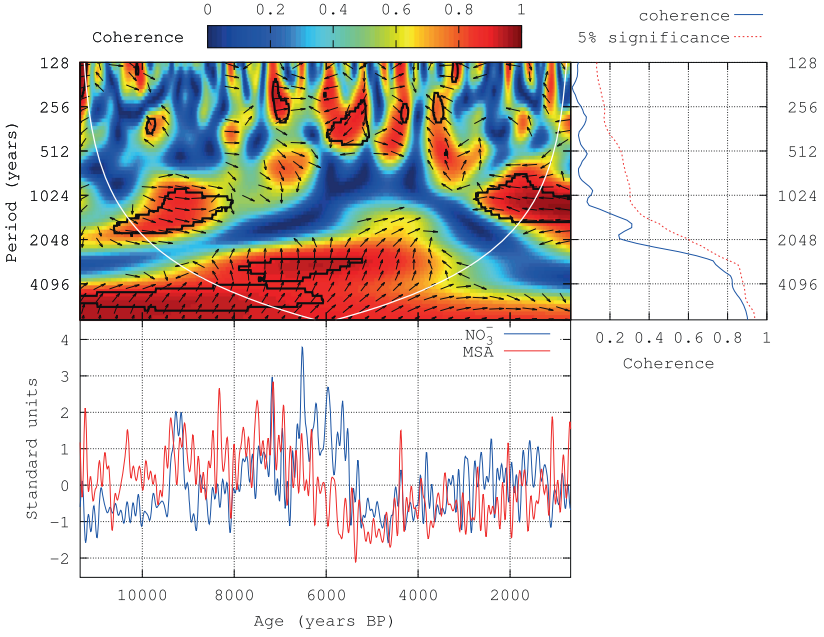

Fig. 5. Similar to Fig. 1 but for the concentrations of $NO_3^{\mathcal{G}}$ and MSA.

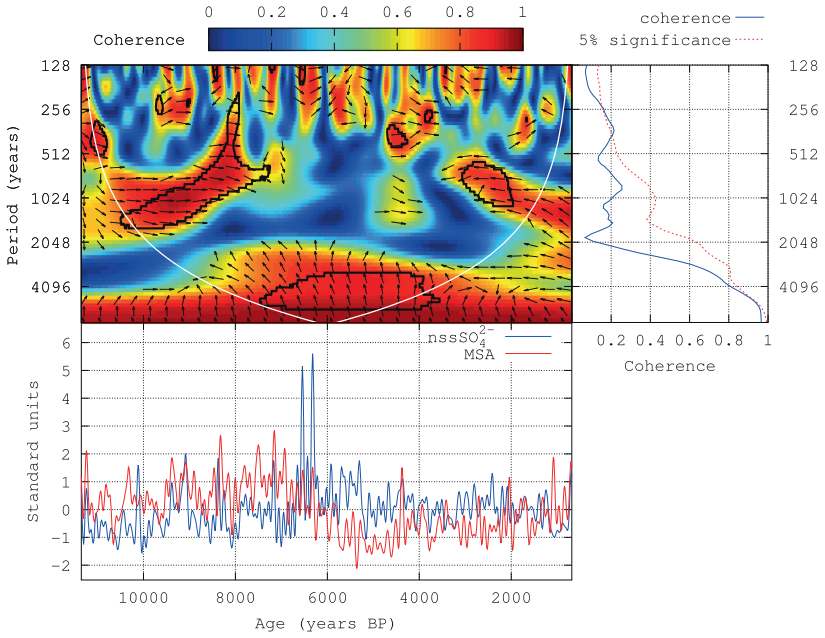

Fig. 6. Similar to Fig. 1 but for the concentrations of no-sea-salt $SO_4^{2\mathcal{G}}$ and MSA.

is localised at 8000–5500 BP and can be divided into two intervals: ca. 2500 BP and ca. 5000 BP. The relative phase is about +90°. One can see in the bottom panel that the increase of $NO_3^{\mathcal{G}}$ at 8000–5000 BP can produce an effect of phase shift against the similar increase of MSA at 10,000–6500 BP. At the mid-period range there are two "spots" (ca. 10,000–8000 and 2500–700 BP) with the opposite phases 0° and 180°. They indicate in- and anti-phase behaviours of the series for the period of about 1200 years. This suggests a lack of the real causal relation between them. Finally, at the short-period range there are a number of short-term "spots" with very variable phases. The pattern of coherence between $NO_3^{\mathcal{G}}$ and MSA does not allow us to conclude that there is any appreciable relation between them. MSA is related to the factors driving the marine biogenic production, likely to be a combination of solar insolation, sea ice extent and favourable atmospheric circulation delivering MSA to the deposition site from the highly productive oceanic areas. Therefore the lack of relation suggests possibly weak, if any, influence of these factors on the $NO_3^{\mathcal{G}}$-record.

Fig. 6 shows a comparison of the $nssSO_4^{2\mathcal{G}}$ and MSA series. The result is very close to that for the $NO_3^{\mathcal{G}}$ vs. MSA comparison. There are three significant "spots" of coherence: one is at long periods at ca. 7500–4000 BP with the relative phase of about 90°, two at middle periods at ca. 10,500–7500 and 3000–2000 BP with phases being about 0° and 180°, respectively. As in the case of the $NO_3^{\mathcal{G}}$ vs. MSA comparison, we conclude that the $nssSO_4^{2\mathcal{G}}$ and MSA series are most likely not related to each other. It can be explained by production through different oxidation mechanisms, involving different intermediates of oxidation (Preunkert et al., 2008). Such a difference is likely to be responsible for their different seasonal temporal pattern, still showing summer maxima and winter minima but exhibiting multiple maxima and a much more variable pattern for MSA with respect to $nssSO_4^{2\mathcal{G}}$. This could be a reason why $NO_3^{\mathcal{G}}$ shows a high and significant coherence with $nssSO_4^{2\mathcal{G}}$ all through the examined period at long periods and in several areas in mid-period range whereas the coherence with MSA (Fig. 5) is more fluctuating and intermittent.

There is one more important reason to consider $NO_3^{\mathcal{G}}$, $nssSO_4^{2\mathcal{G}}$ and MSA — transport of air masses from low and middle latitudes. As mentioned above, transport processes may play a significant role by connecting regions with high $NO_3^{\mathcal{G}}$ productivity in lower latitudes with a polar site of deposition. Since both $nssSO_4^{2\mathcal{G}}$ and MSA are expected to be well connected to each other because they are mainly related to the same origin (phytoplankton activity in the ocean, which represents the only source for MSA and the dominant one for $nssSO_4^{2\mathcal{G}}$ except for the sporadic volcanic inputs, negligible in terms of the $nssSO_4^{2\mathcal{G}}$ budget for timescales of hundreds years and longer) (e.g., Saltzman et al., 1985), one would expect to observe good relation between them in assumption of good air transport from lower latitudes (the ocean surface). However, as one can see in Fig. 5, this is not the case, and we cannot recognize any sign of a stable transport process from this result. In this regard, it has to be noticed that MSA records along the whole TALDICE core show a poor correlation with $nssSO_4^{2\mathcal{G}}$ (unpublished data) and also a scarce correlation was found between atmospheric MSA and $nssSO_4^{2\mathcal{G}}$ levels over the course of spring–summer–fall found in inner Antarctica (Dome C) by Preunkert et al. (2008). Such a lack of significant correlation is likely to be due to different oxidation pathways producing MSA over marine and inland regions. This greatly complicates the relationship between MSA and its gaseous precursor (DMS) and challenges a direct link of MSA in Antarctic ice cores with the biogenic production in the Southern Ocean.

3.3. $NO_3^{\mathcal{G}}$ *vs.* $\delta^{18}O$

Comparison of $NO_3^{\mathcal{G}}$ and $\delta^{18}O$ series is shown in Fig. 7. The long-period coherence between them is about 0.6 but statistically insignificant and in anti-phase. Therefore, the series do not have any considerable long-period relation. The area of the mid- and partly short-period range has three "spots" of high and significant coherence at ages 10,500–9000, 7000–6000 and 4000–3500 BP, with the relative phases varying between 0° and 45°. The "spots" with phases close to 0° are situated near the period of 700 years. It implies a common factor for $NO_3^{\mathcal{G}}$ and $\delta^{18}O$ whose influence strongly varies in time. There is also a small "spot" of relatively high coherence at the period of ↗1500 years at the age of 4500 BP. But since it is very short-term and its phase is about +90° (i.e. delay between the series is about 375 years), this "spot" hardly indicates any real relation. Thus the analysis does not show a consistent correlation between $NO_3^{\mathcal{G}}$ and $\delta^{18}O$.

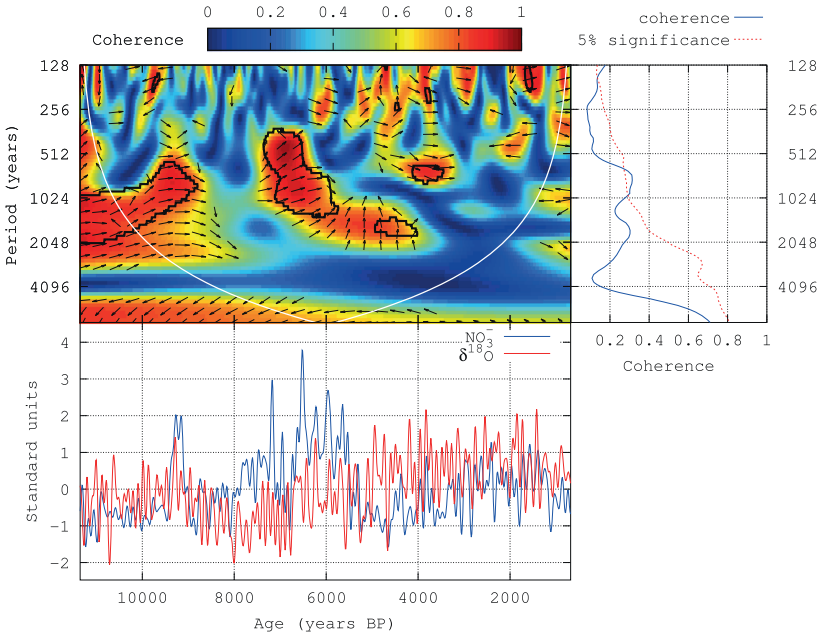

Fig. 7. Similar to Fig. 1 but for the concentration of NO_3^- and $\delta^{18}O$.

Since $\delta^{18}O$ represents the temperature at the site of deposition and is generally related to snow accumulation rate (e.g., Parrenin et al., 2001), its low coherence with NO_3^- suggests that nitrate concentration at Talos Dome during the Holocene is not significantly affected by snow accumulation rate on relatively long (at least decadal, which is the temporal resolution of the samples) timescales.

3.4. NO_3^- vs. Na^+ and Ca^{2+}

The results of comparisons NO_3^- vs. Na^+ and NO_3^- vs. Ca^{2+} are presented in Figs. 8 and 9, respectively. Pairwise coherence is low and insignificant for all period and age ranges except for several small "spots" at the short-period range with floating phase.

The results can be explained by significant differences in processes responsible for generation, transport and deposition of NO_3^-, Na^+ and Ca^{2+}. Na^+ is a component of sea salt aerosol, produced directly above the ocean surface, or via frost flowers formation (Rankin et al., 2000; Schüpbach et al., 2013), or delivered to the deposition site via saline blowing snow (Yang et al., 2008). Calcium ion generally represents dust aerosol travelled from areas with open soil. During Holocene the TALDICE ice core archived dust particles originated not only from Patagonia, South America, but also from regional ice-free areas, namely Northern Victoria Land, East Antarctica (Sala et al., 2008;

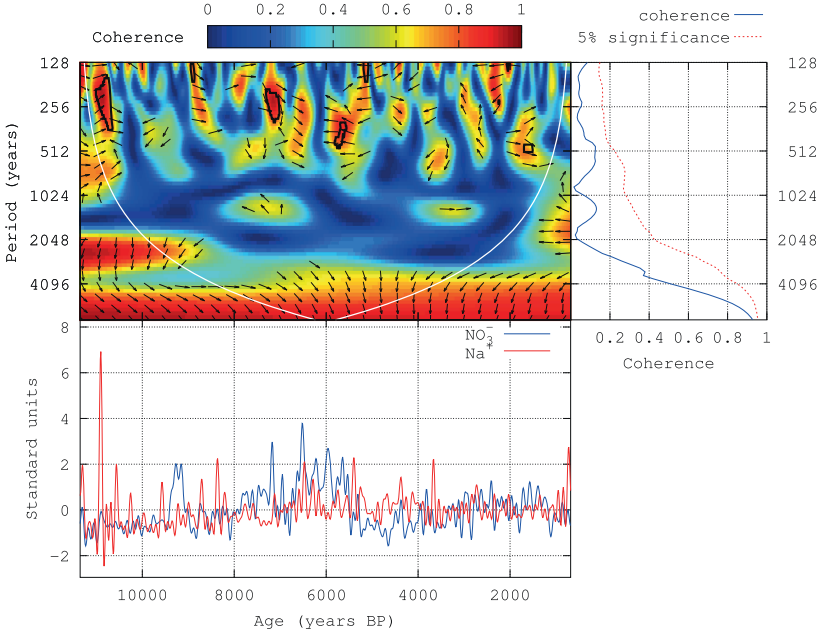

Fig. 8. Similar to Fig. 1 but for the concentrations of NO_3^- and Na^+.

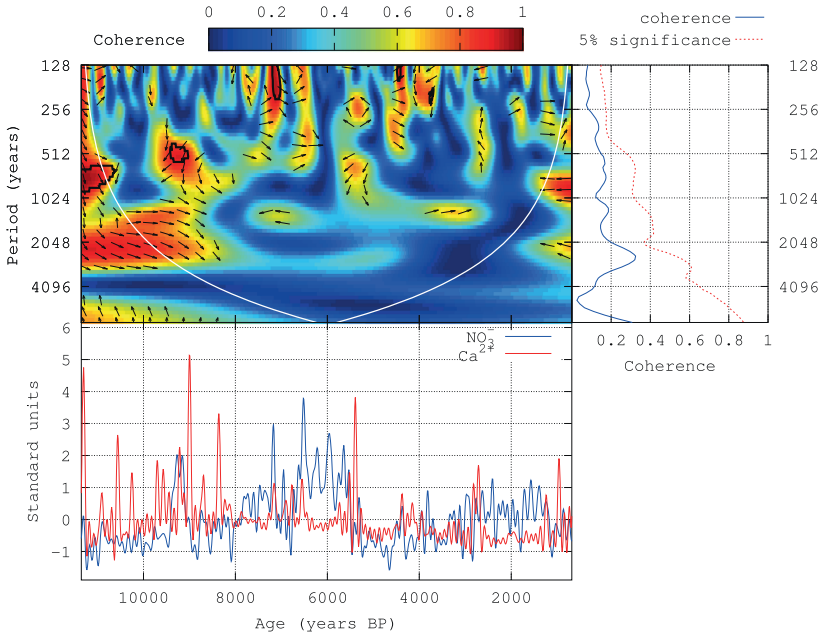

Fig. 9. Similar to Fig. 1 but for the concentrations of NO_3^- and Ca^{2+}.

Table 1
Summary of suggested relations between the series. Three signs in each cell are related to the short, middle and long-term period ranges (see the definitions in Section 3). "+" indicates the presence of significant positive relation between series during the whole time range, "±" indicates the sporadic relation between series, and "−" indicates the lack of any positive relation for a given period range.

	$\Delta^{14}C$	$\Delta^{10}Be$	$nssSO_4^{2-}$	MSA	$\delta^{18}O$	Na^+	Ca^{2+}
NO_3^-	+	±	±	−	±	−	−
$\Delta^{14}C$		±	±	−	±	−	−
$nssSO_4^{2-}$				−			

Delmonte et al., 2010). It might be supposed that common regional transport processes or post-deposition effects could provide some relations among NO_3^-, Na^+ and Ca^{2+} but there are no signs of those in Fig. 8.

4. Conclusions

In this paper we have compared the NO_3^- data series with a number of climatic and cosmic ray indices. The suggested relations between the series are simplistically summed in Table 1.

We found a significant long-period relation of NO_3^- with $\Delta^{14}C$ but not with $\Delta^{10}Be$. In the view of a similar disagreement between $\Delta^{14}C$ and $\Delta^{10}Be$, we conclude that long-period variations of NO_3^- are mainly driven by variability of cosmic ray flux. At mid- and short-period ranges the cosmic ray factor is weak as compared with other factors, as suggested by low coherence of NO_3^- with both $\Delta^{14}C$ and $\Delta^{10}Be$. Comparisons of NO_3^- with climatic proxies yield no significant long-, mid- or short-term relation except for the pair NO_3^- vs. $nssSO_4^{2-}$ that needs a more detailed investigation for interpretation. Assuming a considerable contribution of lightning driven NO_3^- into total deposition, we have searched for signatures of possible air transport from lower latitudes by comparisons of $nssSO_4^{2-}$ and MSA; NO_3^- and Na^+, Ca^{2+}. The results do not show any sign of occurrence of the transport mechanism. Therefore, we suggest that the influence of the lower latitude NO_3^- source at the Talos Dome ice core is weak. Consequently, processes not related to the long-range transport of NO_3^- precursors play a crucial role in its formation in the TALDICE ice core.

This hypothesis needs quantitative estimation of possible effects, thus the further study of NO_3^- in polar regions should be continued by modeling of global and local processes that can influence on it.

Acknowledgements

This work is a contribution to the TALDICE project. TALDICE (Talos Dome Ice Core Project) is a joint European programme, funded by national contributions from Italy, France, Germany, Switzerland and the United Kingdom. Primary logistic support was provided by PNRA at Talos Dome. This is TALDICE publication no. 40. This work was partly done in the framework of the ReSoLVE Center of Excellence (Finnish Academy Project no. 272157).

References

Bazin, L., Landais, A., Lemieux-Dudon, B., Toyé Mahamadou Kele, H., Veres, D., Parrenin, F., Martinerie, P., Ritz, C., Capron, E., Lipenkov, V., Loutre, M.-F., Raynaud, D., Vinther, B., Svensson, A., Rasmussen, S.O., Severi, M., Blunier, T., Leuenberger, M., Fischer, H., Masson-Delmotte, V., Chappellaz, J., Wolff, E., 2013. An optimized multi-proxy, multi-site antarctic ice and gas orbital chronology (aicc2012): 120–800 ka. Clim. Past 9 (4), 1715–1731, URL ⟨http://www.clim-past.net/9/1715/2013/⟩.

Becagli, S., Castellano, E., Cerri, O., Curran, M., Frezzotti, M., Marino, F., Morganti, A., Proposito, A., Severi, M., Traversi, R., Udisti, R., 2009. Methanesulphonic acid (MSA) stratigraphy from a Talos Dome ice core as a tool in depicting sea ice changes and southern atmospheric circulation over the previous 140 years. Atmos. Environ. 43 (5), 1051–1058, URL ⟨http://www.sciencedirect.com/science/article/pii/S1352231008010789⟩.

Beer, J., McCracken, K., von Steiger, R., 2012. Cosmogenic Radionuclides: Theory and Applications in the Terrestrial and Space Environments. Springer, Berlin.

Curran, M.A.J., van Ommen, T.D., Morgan, V.I., Phillips, K.L., Palmer, A.S., 2003. Ice core evidence for antarctic sea ice decline since the 1950s. Science 302 (5648), 1203–1206, URL ⟨http://www.sciencemag.org/content/302/5648/1203.abstract⟩.

Delmas, R.J., 1992. Environmental information from ice cores. Rev. Geophys. 30 (1), 1–21. http://dx.doi.org/10.1029/91RG02725.

Delmonte, B., Baroni, C., Andersson, P.S., Schoberg, H., Hansson, M., Aciego, S., Petit, J.-R., Albani, S., Mazzola, C., Maggi, V., Frezzotti, M., 2010. Aeolian dust in the Talos Dome ice core (East Antarctica, Pacific/Ross Sea sector): Victoria land versus remote sources over the last two climate cycles. J. Quat. Sci. 25 (8), 1327–1337, URL http://dx.doi.org/10.1002/jqs.1418.

Ebisuzaki, W., 1997. A method to estimate the statistical significance of a correlation when the data are serially correlated. J. Clim. 10, 2147–2153.
EPICA Community Members, 2004. Eight glacial cycles from an Antarctic ice core. Nature 429(6992), 623–628. URL ⟨http://nora.nerc.ac.uk/12161/⟩.
Grannas, A.M., Jones, A.E., Dibb, J., Ammann, M., Anastasio, C., Beine, H.J., Bergin, M., Bottenheim, J., Boxe, C.S., Carver, G., Chen, G., Crawford, J.H., Dominé, F., Frey, M. M., Guzmán, M.I., Heard, D.E., Helmig, D., Hoffmann, M.R., Honrath, R.E., Huey, L.G., Hutterli, M., Jacobi, H.W., Klán, P., Lefer, B., McConnell, J., Plane, J., Sander, R., Savarino, J., Shepson, P.B., Simpson, W.R., Sodeau, J.R., von Glasow, R., Weller, R., Wolff, E.W., Zhu, T., 2007. An overview of snow photochemistry: evidence, mechanisms and impacts. Atmos. Chem. Phys. 7 (16), 4329–4373, URL ⟨http://www.atmos-chem-phys.net/7/4329/2007/⟩.
Grinsted, A., Moore, J.C., Jevrejeva, S., 2004. Application of the cross wavelet transform and wavelet coherence to geophysical time series. Nonlinear Process. Geophys. 11, 561–566.
Kepko, L., Spence, H., Smart, D.F., Shea, M.A., 2009. Interhemispheric observations of impulsive nitrate enhancements associated with the four large ground-level solar cosmic ray events (1940–1950). J. Atmos. Sol.-Terr. Phys. 71 (17–18), 1840–1845, URL ⟨http://www.sciencedirect.com/science/article/pii/S1364682609001850⟩.
Kovaltsov, G., Mishev, A., Usoskin, I., 2012. A new model of cosmogenic production of radiocarbon ^{14}C in the atmosphere. Earth Planet. Sci. Lett. 337, 114–120.
Lachaux, J.-P., Lutz, A., Rudrauf, D., Cosmelli, D., Quyen, M.L.V., Martinerie, J., Varela, F., 2002. Estimating the time-course of coherence between single-trial brain signals: an introduction to wavelet coherence. Neurophysiol. Clin. 32 (3), 157–174, URL ⟨http://www.sciencedirect.com/science/article/pii/S0987705302003015⟩.
Legrand, M., Mayewski, P., 1997. Glaciochemistry of polar ice cores: a review. Rev. Geophys. 35, 219–244.
Legrand, M.R., Kirchner, S., 1990. Origins and variations of nitrate in south polar precipitation. J. Geophys. Res. 95 (D4), 3493–3507. http://dx.doi.org/10.1029/JD095iD04p03493.
Mayewski, P.A., Lyons, W.B., Spencer, M.J., Twickler, M., Dansgaard, W., Koci, B., Davidson, C.I., 1986. Sulfate and nitrate concentrations from a south greenland ice core. Science 232 (4753), 975–977.
Mayewski, P.A., Lyons, W.B., Spencer, M.J., Twickler, M.S., Buck, C.F., Whitlow, S., 1990. An ice-core record of atmospheric response to anthropogenic sulphate and nitrate. Nature 346, 554–556.
McCracken, K., Dreschhoff, G., Zeller, E., Smart, D., Shea, M., 2001. Solar cosmic ray events for the period 1561–1994: 1. Identification in polar ice, 1561–1950. J. Geophys. Res. 106, 21585–21598.
Palmer, A.S., Van Ommen, T.D., Curran, M.A.J., Morgan, V., 2001. Ice-core evidence for a small solar-source of atmospheric nitrate. Geophys. Res. Lett. 28 (10), 1953–1956. http://dx.doi.org/10.1029/2000GL012207.
Parrenin, F., Jouzel, J., Waelbroeck, C., Ritz, C., Barnola, J.-M., 2001. Dating the Vostok ice core by an inverse method. J. Geophys. Res. Atmos. 106 (D23), 31837–31851. http://dx.doi.org/10.1029/2001JD900245.
Poluianov, S., Usoskin, I., 2014. Critical analysis of a hypothesis of the planetary tidal influence on solar activity. Sol. Phys. 289 (6), 2333–2342. http://dx.doi.org/10.1007/s11207-014-0475-0.
Preunkert, S., Jourdain, B., Legrand, M., Udisti, R., Becagli, S., Cerri, O., 2008. Seasonality of sulfur species (dimethyl sulfide, sulfate, and methanesulfonate) in Antarctica: inland versus coastal regions. J. Geophys. Res. Atmos. 113 (D15), D15302. http://dx.doi.org/10.1029/2008JD009937.
Rankin, A.M., Auld, V., Wolff, E.W., 2000. Frost flowers as a source of fractionated sea salt aerosol in the polar regions. Geophys. Res. Lett. 27 (21), 3469–3472. http://dx.doi.org/10.1029/2000GL011771.
Reimer, P.J., Baillie, M.G.L., Bard, E., Bayliss, A., Beck, J.W., Blackwell, P.G., Ramsey, C. B., Buck, C.E., Burr, G.S., Edwards, R.L., Friedrich, M., Grootes, P.M., Guilderson, T. P., Hajdas, I., Heaton, T.J., Hogg, A.G., Hughen, K.A., Kaiser, K.F., Kromer, B., McCormac, F.G., Manning, S.W., Reimer, R.W., Richards, D.A., Southon, J.R., Talamo, S., Turney, C.S.M., van der Plicht, J., Weyhenmeye, C.E., 2009. INTCAL09 and Marine09 radiocarbon age calibration curves, 0–50000 years cal BP. Radiocarbon 51 (4), 1111–1150.
Sala, M., Delmonte, B., Frezzotti, M., Proposito, M., Scarchilli, C., Maggi, V., Artioli, G., Dapiaggi, M., Marino, F., Ricci, P., Giudici, G.D., 2008. Evidence of calcium carbonates in coastal (Talos Dome and Ross Sea area) East Antarctica snow and firn: environmental and climatic implications. Earth Planet. Sci. Lett. 271 (1-4), 43–52, URL ⟨http://www.sciencedirect.com/science/article/pii/S0012821X08002045⟩.
Saltzman, E.S., Dioumaeva, I., Finley, B.D., 2006. Glacial/interglacial variations in methanesulfonate (MSA) in the Siple dome ice core, west antarctica. Geophys. Res. Lett. 33 (11), L11811. http://dx.doi.org/10.1029/2005GL025629.
Saltzman, E.S., Savoie, D.L., Prospero, J.M., Zika, R.G., 1985. Atmospheric methanesulfonic acid and non-sea-salt sulfate at fanning and american samoa. Geophys. Res. Lett. 12 (7), 437–440. http://dx.doi.org/10.1029/GL012i007p00437.
Schüpbach, S., Federer, U., Kaufmann, P.R., Albani, S., Barbante, C., Stocker, T.F., Fischer, H., 2013. High-resolution mineral dust and sea ice proxy records from the Talos Dome ice core. Clim. Past 9 (6), 2789–2807, URL ⟨http://www.clim-past.net/9/2789/2013/⟩.
Severi, M., Becagli, S., Castellano, E., Morganti, A., Traversi, R., Udisti, R., 2009. Thirty years of snow deposition at Talos Dome (Northern Victoria Land, East Antarctica): chemical profiles and climatic implications. Microchem. J. 92 (1), 15–20, URL ⟨http://www.sciencedirect.com/science/article/pii/S0026265X08001008⟩.
Soon, W., Velasco Herrera, V.M., Selvaraj, K., Traversi, R., Usoskin, I., Chen, C.-T.A., Lou, J.-Y., Kao, S.-J., Carter, R.M., Pipin, V., Severi, M., Becagli, S., 2014. A review of holocene solar-linked climatic variation on centennial to millennial timescales: physical processes, interpretative frameworks and a new multiple cross-wavelet transform algorithm. Earth Sci. Rev. 134 (0), 1–15, URL ⟨http://www.sciencedirect.com/science/article/pii/S0012825214000518⟩.
Steinhilber, F., Abreu, J.A., Beer, J., 2008. Solar modulation during the Holocene. Astrophys. Space Sci. Trans. 4, 1–6.
Steinhilber, F., Abreu, J.A., Beer, J., Brunner, I., Christl, M., Fisher, H., Heikkilä, U., Kubik, P.W., Mann, M., McCracken, K.G., Miller, H., Miyahara, H., Oerter, H., Wilhelms, F., 2012. 9,400 years of cosmic radiation and solar activity from ice cores and tree rings. Proc. Natl. Acad. Sci. USA 109 (16), 5967–5971.
Torrence, C., Compo, G., 1998. A practical guide to wavelet analysis. Bull. Am. Meteorol. Soc. 79, 61–78.
Traufetter, F., Oerter, H., Fischer, H., Weller, R., Miller, H., 2004. Spatio-temporal variability in volcanic sulphate deposition over the past 2 kyr in snow pits and firn cores from Amundsenisen, Antarctica. J. Glaciol. 50 (168), 137–146, URL ⟨http://www.ingentaconnect.com/content/igsoc/jog/2004/00000050/00000168/art00014⟩.
Traversi, R., Becagli, S., Castellano, E., Largiuni, O., Migliori, A., Severi, M., Frezzotti, M., Udisti, R., 2004. Spatial and temporal distribution of environmental markers from coastal to plateau areas in Antarctica by firn core chemical analysis. Int. J. Environ. Anal. Chem. 84 (6-7), 457–470.
Traversi, R., Usoskin, I.G., Solanki, S.K., Becagli, S., Frezzotti, M., Severi, M., Stenni, B., Udisti, R., 2012. Nitrate in polar ice: a new tracer of solar variability. Sol. Phys. 280, 237–254.
Usoskin, I.G., 2013. A history of solar activity over millennia. Living Rev. Sol. Phys. 10 (1), URL ⟨http://www.livingreviews.org/lrsp-2013-1⟩.
Usoskin, I.G., Alanko-Huotari, K., Kovaltsov, G.A., Mursula, K., 2005. Heliospheric modulation of cosmic rays: monthly reconstruction for 1951–2004. J. Geophys. Res. 110, A12108.
Usoskin, I.G., Horiuchi, K., Solanki, S., Kovaltsov, G.A., Bard, E., 2009. On the common solar signal in different cosmogenic isotope data sets. J. Geophys. Res. Space 114 (A3), A03112. http://dx.doi.org/10.1029/2008JA013888, URL ⟨http://www.livingreviews.org/lrsp-2013-1⟩.
Usoskin, I.G., Solanki, S.K., Kovaltsov, G.A., 2007. Grand minima and maxima of solar activity: new observational constraints. Astron. Astrophys. 471, 301–309.
Usoskin, I.G., Voiculescu, M., Kovaltsov, G.A., Mursula, K., 2006. Correlation between clouds at different altitudes and solar activity: fact or artifact?. J. Atmos. Sol.-Terr. Phys. 68, 2164–2172.
Vitt, F.M., Jackman, C.H., 1996. A comparison of sources of odd nitrogen production from 1974 through 1993 in the earth's middle atmosphere as calculated using a two-dimensional model. J. Geophys. Res. Atmos. 101 (D3), 6729–6739. http://dx.doi.org/10.1029/95JD03386.
Vonmoos, M., Beer, J., Muscheler, R., 2006. Large variations in holocene solar activity: constraints from ^{10}Be in the greenland ice core project ice core. J. Geophys. Res. 111 (A10), A10105.
Weller, R., Wagenbach, D., 2007. Year-round chemical aerosol records in continental antarctica obtained by automatic samplings. Tellus B 59 (4), 755–765. http://dx.doi.org/10.1111/j.1600-0889.2007.00293.x.
Wolff, E.W., 1995. Nitrate in polar ice. In: Delmas, R.J. (Ed.), Ice Core Studies of Global Biogeochemical Cycles. NATO ASI Series, vol. 30. Springer, Berlin, Heidelberg, pp. 195–224. http://dx.doi.org/10.1007/978-3-642-51172-1_10.
Wolff, E.W., Bigler, M., Curran, M.A.J., Dibb, J.E., Frey, M.M., Legrand, M., McConnell, J.R., 2012. The Carrington event not observed in most ice core nitrate records. Geophys. Res. Lett. 39, L08503.
Wolff, E.W., Jones, A.E., Bauguitte, S.J.-B., Salmon, R.A., 2008. The interpretation of spikes and trends in concentration of nitrate in polar ice cores, based on evidence from snow and atmospheric measurements. Atmos. Chem. Phys. 8 (18), 5627–5634, URL ⟨http://www.atmos-chem-phys.net/8/5627/2008/⟩.
Yang, X., Pyle, J.A., Cox, R.A., 2008. Sea salt aerosol production and bromine release: Role of snow on sea ice. Geophys. Res. Lett. 35 (16), L16815. http://dx.doi.org/10.1029/2008GL034536.
Yiou, F., Raisbeck, G., Baumgartner, S., Beer, J., Hammer, C., Johnsen, S., Jouzel, J., Kubik, P., Lestringuez, J., Stiévenard, M., Suter, M., Yiou, P., 1997. Beryllium 10 in the greenland ice core project ice core at summit, Greenland. J. Geophys. Res. 102, 26783–26794.